Synthesis of Temperature Responsive Biohybrid Guar-Based Grafted Copolymers by Click Chemistry

ARTICLE *in* MACROMOLECULES · AUGUST 2010

Impact Factor: 5.8 · DOI: 10.1021/ma101215d · Source: OAI

Macromolecules
ARTICLE

Macromolecules **2010**, *43*, 6843–6852 **6843**
DOI: 10.1021/ma101215d

Synthesis of Temperature Responsive Biohybrid Guar-Based Grafted Copolymers by Click Chemistry

Morgan Tizzotti,[†,‡] Caroline Creuzet,[†,‡] Marie-Pierre Labeau,[‡] Thierry Hamaide,[†] Fernande Boisson,[†] Eric Drockenmuller,[†] Aurélia Charlot,*[,†] and Etienne Fleury*[,†]

[†]*Université de Lyon, F-69361, Lyon, France, CNRS, UMR 5223, Ingénierie des Matériaux Polymères, F-69621, Villeurbanne, France, INSA Lyon, F-69621, Villeurbanne, France, Université Claude Bernard Lyon 1, F-69622, Villeurbanne, France, and* [‡]*Rhodia Bristol Research & Technical Center, 350 George Patterson Boulevard, Bristol, Pennsylvania 19007*

Received June 1, 2010; Revised Manuscript Received July 8, 2010

ABSTRACT: Novel thermoresponsive biohybrid guar-based grafted copolymers were prepared in aqueous medium by copper catalyzed 1,3-dipolar Huisgen cycloaddition between an α-butoxy-ω-azido-PEO-*co*-PPO derivative, characterized by LCST behavior, and guar gum bearing alkyne functionalities randomly distributed along the chain. The chemical pathway gives well-defined guar-*g*-(PEO-*co*-PPO) copolymers with tunable chemical compositions. The resulting grafted copolymers were shown to exhibit a reversible thermo-induced association leading to elastic physical network-like behaviors. It has been shown that the rheological properties are intimately related to the molecular weight and to the degree of substitution of guar. The temperature of association of the grafted copolymer is controlled by the cloud point of the grafted polyoxyalkylene and the salt concentration variation appeared as a very convenient manner to tune the thermoresponsive character without changing the chemical nature of the side-chains. Finally, in relation with macroscopic properties, the thermoassociative effect was monitored by NMR analysis.

Introduction

Thermally responsive systems based on polymers which exhibit a lower critical solution temperature (LCST) have gained interest during the last 15 years and have demonstrated their capability for peculiar applications, as cosmetics, oil recovery,[1−3] but also in biomedical fields as drug release[4] or tissue engineering.[5] In particular, water-soluble grafted copolymers have appeared as good candidates and can undergo a well tailored thermo-induced and reversible sol−gel transition. Several works described the generation of "all-synthetic" thermoassociative grafted copolymers based on hydrophilic backbone, made of poly(sodium acrylate),[6−9] poly(acrylamide),[10,11] poly(phosphazene) derivatives,[12,13] or poly(ethylene oxide)[14,15] bearing either thermosensitive poly(*N*-isopropylacrylamide) (PNIPAAm) or polyoxyalkylene copolymers. Design of thermoassociative "biohybrid" grafted copolymers from polysaccharide as backbone is becoming a very interesting tool because the resulting systems can combine the performances of natural polymers, such as hydrophilicity, viscoelastic properties, biodegradability,and biocompatibility with the responsive behavior of synthetic segments. In this frame, the used polysaccharides are chitosan,[16−21] hyaluronane,[22−24] carboxymethylcellulose,[25−27] alginate,[27] and dextran[27] functionalized by PNIPAAm or poly(ethylene oxide-*co*-propylene oxide) (PEO-*co*-PPO) side-chains. The synthesis of such thermosensitive biohybrid copolymers included either (i) the "grafting from" pathway by conventional radical[16,17,22] and controlled radical polymerization (CRP)[28] with mainly the use of atom transfer radical polymerization and reversible addition−fragmentation chain transfer or (ii) the "grafting onto" route occurring through coupling chemical reactions such as peptidic-like coupling,[16,18,21,23−27] or reductive amination.[19−21] These pathways are not quantitative and are sensitive to the molecular weight of the polysaccharide,[27] and some of them occur in organic medium.

Guar gum is a relevant building-block for the development of responsive biohybrid copolymer due to its easy availability, low cost and ability to form viscous solutions and physical gels at low concentration in water. Guar is a water-soluble nonionic polysaccharide extracted from the seeds of *Cyamopsis tetragonoloba*, constituted by a β-1,4-mannose backbone with randomly distributed α-1,6-galactose side chains. The mannose/galactose ratio is generally between 1.3 and 1.8.[29] It is widely employed in the food, paper, textile, petroleum, personal care, and biomaterial industries.[30−37]

Conversion of guar to its guar-*g*-(PEO-*co*-PPO) derivative has already been described.[2] However, it was based on three steps: that is, guar carboxymethylation with sodium chloroacetate, followed by an esterification with dimethyl sulfate to afford a reactive derivative toward amino groups, and then an amidation reaction of esterified guar with a series of amino functionnalized polyoxyalkylenes. This latter amidification coupling was performed under aggressive conditions (DMSO, 95 °C, 24−48 h), leading to guar chain degradation. Additionally, it was shown to strongly depend on the polyoxyalkylene molecular weight and led to very low yields and low conversions. Consequently, an efficient, selective and especially non degradable aqueous synthetic route for the preparation of thermoresponsive guar-based grafted copolymers with high yields, is still lacking. Also, the preparation of well-defined grafted copolymers is essential for a good control of the resulting rheological properties.

With respect to these requirements, we describe the synthesis of novel thermoresponsive biohybrid grafted copolymers by exploiting the efficient, versatile, and robust copper-catalyzed azide−alkyne Huisgen cycloaddition (CuAAC) to graft PEO-*co*-PPO onto guar chain backbones. This synthetic pathway has

*Corresponding author. E-mail: (A.C.) aurelia.charlot@insa-lyon.fr; (E.F.) etienne.fleury@insa-lyon.fr.

Published on Web 07/23/2010

been shown particularly efficient for the chemical modification of polysaccharides to obtain biohybrid systems.[38] The preparation of the targeted grafted copolymers involved the conversion of α-butoxy-ω-hydroxy-PEO-*co*-PPO, characterized by LCST behavior into its α-butoxy-ω-azido derivative in order to be selectively grafted on a guar derivative possessing pendant alkyne functionalities along the chain. The purposes are to establish a closely structure−property relationship in term of thermoresponsive rheological behavior and to investigate the influence of external parameters on the association process.

Experimental Section

Materials. Three guar gums (**4$_a$**, M_w = 58 kg/mol, I_p = 2.21; **4$_b$**, M_w = 126 kg/mol, I_p = 1.92; **4$_c$**, M_w = 299 kg/mol, I_p = 1.82) were provided by Rhodia (ratio mannose/galactose ≈ 1.3). α-Butoxy-ω-hydroxy-poly[(ethylene oxide)-*co*-(propylene oxide)] (denoted ω-OH-PEO-*co*-PPO) having a 1:1 molar ratio of PEO and PPO units (Dow, M_n = 1600 g/mol, I_p = 1.2) and α-methoxy-ω-hydroxy-poly(ethylene glycol) (PEG) (denoted PEG) (Aldrich, M_n = 350 g/mol) were dried by azeotropic distillation of toluene before use. Sodium hydroxide (98%), propargyl bromide (80% in toluene), sodium L-ascorbate (≥98%), copper(II) sulfate pentahydrate (99.995%), sodium azide (99.99%), methanesulfonyl chloride (99.7%), triethylamine (99.5%), sodium benzoate (99%), tetramethylsilane (TMS, ≥ 99.9%), 3-(trimethylsilyl)-propionic acid-d_4 sodium salt (TSPD$_4$, 98%) and anhydrous tetrahydrofuran (THF, 99.9%) were purchased from Aldrich and used as received. 2-Propanol (99%), toluene (99%), methylene chloride (99%), *N,N*-dimethylformamide (DMF, 99%), deuterium oxide (99.9 atom % D) and deuterated chloroform (99.9 atom % D) were purchased from SDS and used as received. α-Methoxy-ω-azido−PEG with M_n = 350 g/mol was synthesized according to a previously described synthetic procedure.[39] Water used was ultrapure (from UHQ II) with a resistivity of approximately 18 μS/cm.

Characterization Methods. ^{1}H NMR spectra were recorded with a 5 mm QNP probe on a Bruker Avance II spectrometer in D_2O at 70 °C (10 mg/mL, 512 scans, 250 MHz) using TSPD$_4$ as reference for chemical shifts (0 ppm) or in $CDCl_3$ at room temperature (10 mg/mL, 32 scans, 250 MHz) using TMS as reference for chemical shifts (0 ppm). ^{13}C NMR spectra were recorded with a 5 mm QNP probe on a Bruker DRX400 Spectrometer in $CDCl_3$ at room temperature (100 mg/mL, 1024 scans, 100 MHz) using TMS as reference for chemical shifts (0 ppm).

For temperatures higher than room temperature, the tubes were left to stabilize for 15 min at the desired temperature before recording the spectrum.

For the 2D NMR HMBC experiments recorded on alkyne-functionalized guars, a 5 mm broad band probe with pulse field gradient on the *z*-axis was used. PFG-HMBC sequence was used for ^{1}H−^{13}C correlations. The spectra were acquired with a relaxation delay of 2 s, 0.20 s acquisition time, a delay of Δ = 1/2, $^1J_{CH}$ = 3.5 ms for one-bond correlation suppression and a delay of Δ = $^1/_2$, $^nJ_{CH}$ = 60 ms (average $^nJ_{CH}$ = 8.3 Hz) for long-range correlations. Details concerning experimental conditions are given in the figure captions.

TGA measurements were performed under nitrogen using a TA Instruments TGA Q500 apparatus at a heating rate of 10 °C/min.

FTIR spectra were recorded using KBr pellets with a Magna-IR Nicolet 550 collecting 32 scans from 500 to 4000 cm^{-1}, KBr pellets for solid samples were prepared by grinding the sample with solid potassium bromide (KBr) and applying pressure (10 tons) during 10 min to the dry mixture.

SEC measurements of PEO-*co*-PPO derivatives were performed using a Wyatt instrument consisting of a pump, a refractive index detector and two PL gel-mixed columns (E30 and E03). THF was used as the eluent at a flow rate of 0.7 mL/min at 25 °C. Data analyses were performed with ASTRA 5.3.1 software.

For SEC measurements of guar dispersed in basic hydroalcoholic medium, the samples were dissolved in the mobile phase (aqueous solution of ammonium acetate at 0.15 M/acid acetic buffer 0.2 M pH = 4.5) at 0.1% wt and filtered through 0.45 μm cellulose filters (Millipore) prior to injection. Samples were analyzed with a detector MALLS Waters R410 (working at 632.8 nm, Wyatt Dawn DSP). The SEC device is also composed by an IsoChrom LC pump (Spectra Physics) connected to 1 column Protein Pack glass 200 SW and 1 column TSK gel 6000 PW used in series. d*n*/d*c* is fixed at 0.15 for guar. Acquisitions were performed at ambient temperature at a flow rate of 0.5 mL/min.

The LCST values of solutions of α-butoxy-ω-hydroxy-PEO-*co*-PPO and of its α-butoxy-ω-azido derivative (at 1 wt % in water) were determined by turbidity measurements. The experiments consisted in exposing the copolymer solution to a polychromatic white light and in monitoring the total transmitted light through the sample over the whole wavelength range as a function of the temperature. The sample was placed in a thermostated vat and heated with a heating rate of 1 °C/min.

The viscosity analysis as well as the viscoelastic properties of aqueous solutions of guar copolymers were carried out on a AR1000 controlled stress rheometer (TA Instruments Inc., U.K.) using an aluminum cone/plate geometry (diameter 60 mm, angle 2°, gap 2 μm), operating in flow or dynamic mode, respectively. All the dynamic rheological data were checked as a function of strain amplitude to ensure that the measurements were performed in the linear viscoelastic region. The temperature was precisely controlled by a high power Peltier system. The dissolution time of each guar derivative was at least 12 h at room temperature in distilled water under stirring until homogeneous solutions were obtained. Samples were then left to equilibrate 24 h prior to analyses. A particular care was taken in order to prevent water evaporation during measurements at high temperature by using a homemade cover combined to the deposition of a film of silicone oil on the edges of the sample.

Nomenclature. Alkyne-functionalized guars are denoted **5$_{a,x}$**, **5$_{b,y}$**, and **5$_{c,z}$** and guar-based grafted copolymers are denoted **6$_{a,x'}$**, **6$_{b,y'}$** and **6$_{c,z'}$**. a, b, and c stand for the guar weight-average molar mass (M_w = 58, 126, and 299 kg/mol, respectively). *x*, *y*, and *z* stand for the degree of substitution of guar in alkyne functionalities (DS$_{alkyne}$), and *x*′, *y*′, and *z*′ correspond to the DS of guar in PEO-*co*-PPO side-chains, i.e., the average number of alkyne functionalities or grafted PEO-*co*-PPO side-chains per one anhydro hexose unit determined by ^{1}H NMR spectroscopy and thermogravimetric analysis, respectively.

General Procedure for Alkyne Functionalization of Guar Gums. Synthesis of 5$_{a0.13}$. Guar gum powder **4$_a$** (6.0 g, 110 mmol of hydroxyl groups) was dispersed in 2-propanol (100 mL) and stirred at room temperature for 10 min. An aqueous solution of sodium hydroxide (5 wt %, 31 mL, 39 mmol) was added dropwise, and after 1 h, propargyl bromide (17 g, 110 mmol) was added dropwise before stirring for 1.5 h at 60 °C. After filtration, the solid phase was dissolved in 100 mL of water and precipitated twice in 500 mL of 2-propanol. Solid phase was filtered and dried under vacuum at 30 °C for 18 h. Alkyne functionalized guar **5$_{a0.13}$** was recovered as a slightly yellow powder (5.42 g, 90.3%). FTIR: $\nu_{sC\equiv C}$ = 2120 cm^{-1}. ^{1}H NMR (D_2O) δ (ppm): 5.05 (s, galactose anomeric proton, 1H), 4.75 (s, mannose anomeric proton, 1H), 4.3−4.6 (C**H$_2$**−C≡CH, 2H), 4.25−3.45 (m, H from anhydro hexose units), 2.26−2.14 (bs, C≡C**H**, 1H).

General Procedure for the Determination of the Degree of Substitution of Guar in Alkyne Functionalities DS$_{alkyne}$. The DS of guar in alkyne functionalities (DS$_{alkyne}$) is determined after CuAAc coupling of alkyne functionalized guar with a short α-methoxy-ω-azido-PEG (ω-N$_3$−PEG) involving the total conversion of alkyne groups into triazole rings. The protons from triazole rings are well identified on the ^{1}H NMR spectra

Scheme 1. Alkyne Functionalization of Guar 5

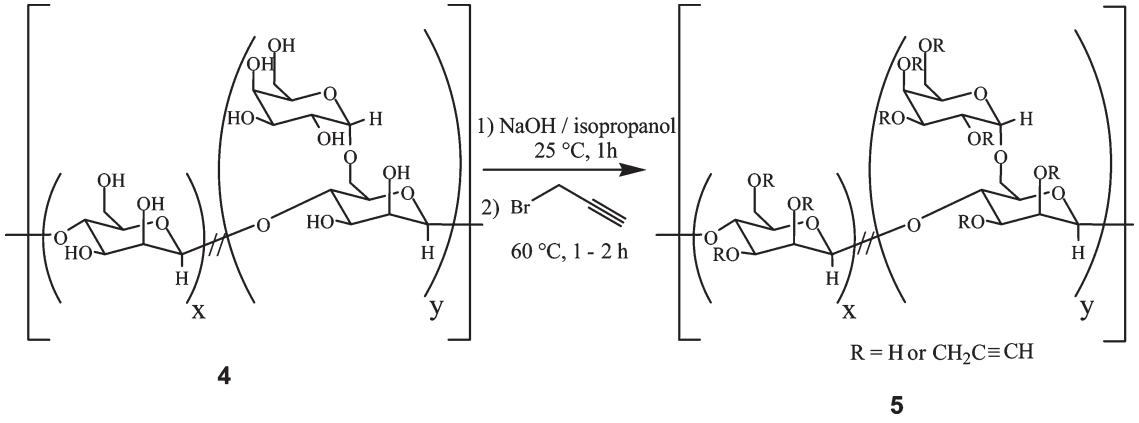

(Figure S4). A large excess of ω-N_3 PEG is used in order to convert all the alkyne groups. The click grafting reaction was performed as followed.

As a typical procedure, 200 mg of alkyne functionalized guar $\mathbf{5}_a$ was dissolved in 8 mL of water. A freshly prepared sodium ascorbate solution (10 wt % in water, 2.4 g, 1.23 mmol), ω-N_3 PEG (350 g/mol, 430 mg, 1.23 mmol) and a freshly prepared copper(II) sulfate pentahydrate solution (1 wt % in water, 1.54 mL, 0.0615 mmol) were sequentially added. The reaction mixture was stirred in the dark for 24 h at 45 °C and the solution was dialyzed during 3 days against water using a cellulose dialysis bag (Orange Scientific, MWCO: 3500 g/mol) to remove catalyst and unreacted excess of ω-N_3−PEG. Water was changed three times a day. The solution was then freeze-dried to yield a yellow solid (221 mg, 90.9%). δ (ppm): ^{1}H NMR (D_2O) δ (ppm): 8.09 (bs, C═C**H**N triazole ring 1 **H**), 7.99−7.41 (m, sodium benzoate 5 aromatic **H**), 5.05 (s, galactose anomeric proton, 1H), 4.8−4.5 (bs, C**H**$_2$CHN triazole, 2H), 4.70 (b, C**H**$_2$N triazole, 2H), 4.75 (s, mannose anomeric proton, 1H), 4.25−3.45 (m, H from anhydro hexose units), 4.05 (−O−C**H**$_2$C**H**$_2$N triazole, 2H), 3.74−3.60 (m, C**H**$_2$C**H**$_2$O of PEG chains, 4*n*H), 3.38 (s, C**H**$_3$O, 3H).

The DS of guar in PEG side-chains were calculated by using the integration of the resulting proton signal of the triazole ring and the integration of aromatic protons of sodium benzoate added in the NMR tube as an external reference. All details are given in the Supporting Information (Figure S4).

Via this method, the estimated DS_{alkyne} values are equal to 0.060 ± 0.006, 0.13 ± 0.01 and 0.20 ± 0.02 which give access to samples $\mathbf{5_{a0.06}}$, $\mathbf{5_{b0.06}}$, $\mathbf{5_{b0.13}}$, $\mathbf{5_{b0.20}}$, $\mathbf{5_{c0.06}}$, $\mathbf{5_{c0.13}}$ and $\mathbf{5_{c0.20}}$. For the synthesis of $\mathbf{5_{a0.06}}$, $\mathbf{5_{b0.06}}$ and $\mathbf{5_{c0.06}}$, the same chemical route was used and was based on a reaction time of 1 h. $\mathbf{5_{b0.13}}$ and $\mathbf{5_{c0.13}}$ result from a reaction time of 1.5 h and for $\mathbf{5_{b0.20}}$ and $\mathbf{5_{c0.20}}$, the reaction time used was 2 h. For all samples, the DS_{alkyne} were determined according the same methodology, i.e. after CuAAC coupling with a ω-N_3−PEG derivative.

Synthesis of α-Butoxy-ω-azido-poly[(ethylene oxide)-*co*-(propylene oxide)] (ω-N_3−PEO-*co*-PPO), 3. Methanesulfonyl chloride (2.37 g, 20.6 mmol) and triethylamine (2.03 g, 20.0 mmol) were added dropwise to a solution of α-butoxy-ω-hydroxy-PEO-*co*-PPO (1600 g/mol, 16.0 g, 10.0 mmol) in anhydrous THF (200 mL) maintained at 0 °C under argon. The mixture was stirred for 24 h at room temperature before filtration of the triethylammonium salt and evaporation of the solvent. The crude product was then dissolved in 200 mL of methylene chloride and successively washed with 200 mL of HCl_{aq} (1 M), 200 mL of $NaOH_{aq}$ (1 M) and 200 mL of $NaCl_{aq}$ (1 M). The organic phase was dried over magnesium sulfate and evaporated under vacuum. The crude α-butoxy-ω-mesylate-PEO-*co*-PPO was then dissolved in 100 mL of DMF and sodium azide (0.97 g, 14.9 mmol) was added. The reaction mixture was stirred in the dark for 24 h at 60 °C before evaporation of DMF at 50 °C under vacuum. The resulting oil was dissolved in 200 mL of methylene chloride and the solution was washed with 100 mL of $NaCl_{aq}$ (1 M). After evaporation of the solvent **3** was obtained as a slightly yellow oil (14.8 g, 92.5%). ^{1}H NMR ($CDCl_3$) δ (ppm): 4.05−3.15 (bm, C**H**$_2$C**H**$_2$O, C**H**$_2$C**H**(CH$_3$)O, C**H**$_2$C**H**(CH$_3$)N$_3$, C**H**(CH$_3$)C**H**$_2$N$_3$, C**H**$_2$C**H**$_2$N$_3$, 17H), 1.48−0.66 (bm, CH$_2$CH-(C**H**$_3$)O, CH$_2$CH(C**H**$_3$)N$_3$, CH(C**H**$_3$)CH$_2$N$_3$, 9H). ^{13}C NMR ($CDCl_3$) δ (ppm): 75.4−67.1 (**C**H$_2$**C**H$_2$O, **C**H$_2$**C**H(CH$_3$)O, **C**H$_2$CH(CH$_3$)N$_3$, **C**H(CH$_3$)CH$_2$N$_3$, **C**H$_2$CH$_2$N$_3$), 56.7−55.9 (CH$_2$**C**H(CH$_3$)N$_3$, CH(CH$_3$)**C**H$_2$N$_3$, CH$_2$**C**H$_2$N$_3$), 17.1−16.1 (CH$_2$CH(**C**H$_3$)O), 15.8−15.5 (CH$_2$CH(**C**H$_3$)N$_3$, CH(**C**H$_3$)-CH$_2$N$_3$). FTIR: ν_{sN3} = 2100 cm^{-1}.

General Procedure for the Synthesis of Guar-Based Grafted Copolymers by Click Chemistry. Synthesis of $\mathbf{6_{b0.12}}$. Alkyne functionalized guar $\mathbf{5_{b0.13}}$ (978 mg, 0.750 mmol of alkyne functionnalities) was dissolved in 100 mL of water. A freshly prepared sodium ascorbate solution (10 wt % in water, 1.2 g, 0.6 mmol) and **3** (965 mg, corresponding to 0.6 mmol of azide functionnalities) were added and the mixture was stirred in the dark at room temperature for 10 min. A freshly prepared copper(II) sulfate pentahydrate solution (1 wt % in water, 750 mg, 0.03 mmol) was added and the mixture was stirred at room temperature during 72 h. The solution was then dialyzed during 3 days against water using a cellulose dialysis bag (Orange Scientific, MWCO: 3500 g/mol) to remove catalyst and eventual unreacted ω-N_3−PEO-*co*-PPO **3** chains. NaN_3 was added to water (10 mg/L) in order to prevent any bacterial degradation. The solution was then freeze-dried to yield a yellow solid (1.76 g, 90.6%). δ (ppm): ^{1}H NMR (D_2O) δ (ppm): 8.09 (bs, C═C**H**N triazole ring, 1 H), 5.05 (s, galactose anomeric proton, 1 H), 4.97−4.47 (m, C**H**$_2$−triazole−C**H**$_2$, 4H), 4.75 (s, mannose anomeric proton, 1 H), 4.25−3.45 (m, H from anhydro hexose units), 3.53 (bs, C**H**$_2$C**H**$_2$O, C**H**$_2$C**H**(CH$_3$)O, (4*n* + 3*m*) H), 1.62−1.42 (m, CH$_3$CH$_2$C**H**$_2$CH$_2$O, 2H), 1.42−1.24 (m, CH$_3$C**H**$_2$CH$_2$CH$_2$O, 2H), 1.16 (m, CH$_2$CH(C**H**$_3$)O, 3*m*H), 0.91 (t, C**H**$_3$CH$_2$CH$_2$-CH$_2$O, 3H). The other grafted guar-based copolymers were prepared using the same procedure, maintaining an alkyne/azide/Na−ascorbate/Cu^{2+} molar ratio of 1.2:1:1:0.05. The DS of guar in PEO-*co*-PPO side-chains were calculated from TGA measurements by using the (PEO-*co*-PPO/guar) weight ratio. The details are given in the Supporting Information (Figure S8).

Results and Discussion

Synthesis and Characterization of the Guar-Based Grafted Copolymers via CuAAc Coupling. On the basis of a chemical pathway previously described with α,ω-diazido-PEO-*co*-PPO,[40] the strategy used to obtain well-defined thermosensitive guar-based grafted copolymers relies on the functionalization of both guar chains by alkyne groups and PEO-*co*-PPO by azide functionalities prior to their coupling through CuAAc coupling. The aqueous medium combined to low temperatures used for both guar functionalization and click

coupling are suitable mild conditions to maintain the integrity of guar chains.

Alkyne Functionalization of Guar. Alkyne functionalities were randomly introduced onto guar chains $\mathbf{4_{a-c}}$ through an alkylation reaction with propargyl bromide from swollen guar particles in basic hydroalcoholic solution (Scheme 1). This functionalization required an optimal NaOH concentration because a weak concentration does not ensure a good swelling and a too high NaOH concentration induces aggregation of the guar particles. The suitable range of NaOH concentration varies between 5 and 10 wt %. These NaOH concentration conditions reduce the guar association by hydrogen interaction through the formation of alcoolate functionalities, which induce the swelling of the guar and the diffusion of the reactive within the swollen guar particles. Thus, the alkyne functionalization of guar chains is assumed to be homogeneous.

1D (^{13}C NMR and DEPT 135) and 2D (HMBC) NMR experiments provided evidence for the conjugation of propargyl bromide on the hydroxyl groups of guar (Figures S1, S2, and S3 in the Supporting Information). The experiments were performed at 70 °C in order to (i) displace the water signal and (ii) to promote the overall mobility to obtain relatively well-defined proton signals. The spectra show a statistical alkylation which concomitantly occurs on both primary and secondary hydroxyl functions of galactose (on G3, G4, and G6 positions) of guar chains. No correlation with hydroxyl of mannose is observed but it does not mean that mannose is not substituted since nearly no correlation related to mannose nucleus is detected with our acquisition parameters. This can be probably due to a lower mobility of the mannose main chain units against the branched galactose ones.

The C≡CH groups of alkyne guars **5** are poorly solvated and thus hardly distinguishable by NMR in D_2O which prevents from a precise and direct determination of DS_{alkyne}. The strategy that we used consisted in totally converting alkyne functionalities into triazole rings after quantitative CuAAc coupling with an excess of hydrophilic ω-N_3−PEG, (M_n = 350 g/mol). The DS_{alkyne} values are assumed to be equal to the DS in PEG side-chains (Figure S4, Supporting Information). The DS_{alkyne} estimated from this method are 0.060 ± 0.006, 0.13 ± 0.01 and 0.20 ± 0.02. The DS_{alkyne} variations were obtained by a modulation of the reaction time from 1 to 2 h. SEC traces of different guar samples $\mathbf{4_a}$ dispersed in basic hydroalcoholic medium show no guar chain degradation in these experimental conditions, contrary to a time of 24 h (Figure S5). The alkylation procedure was applied to guar gum with different molecular weight: $\mathbf{5_a}$, $\mathbf{5_b}$, and $\mathbf{5_c}$ corresponding to M_w = 58 kg/mol, M_w = 126 kg/mol, and M_w = 299 kg/mol, respectively. The nomenclature used for guar derivatives is described in the experimental part. It was shown that the DS values could be also modulated by varying NaOH solution concentration or propargyl bromide amount.[3]

Synthesis of α-*Butoxy-ω-azido-PEO-co-PPO*. The thermosensitive precursor α-butoxy-ω-hydroxy−PEO-*co*-PPO (denoted ω-OH−PEO-*co*-PPO) **1** is a 1600 g/mol 1/1 random copolymer of ethylene oxide and propylene oxide having a LCST or cloud point of ca. 50 °C in water, which was verified by experimental turbidity measurements. The conversion of α-butoxy-ω-hydroxy-PEO-*co*-PPO into its α-butoxy-ω-azido-PEO-*co*-PPO (denoted ω-N_3−PEO-*co*-PPO) derivative was obtained by mesylation and subsequent nucleophilic substitution of the mesylate groups by NaN_3 in DMF instead of water as described for azide functionalization of PEG.[39] The reaction in water solution was shown to

Scheme 2. Synthesis of Guar-*g*-(PEO-*co*-PPO) $\mathbf{6_{a,b,c}}$ by CuAAC between Alkyne-Functionalized Guars $\mathbf{5_{a,b,c}}$ and ω-N_3−PEO-*co*-PPO 3

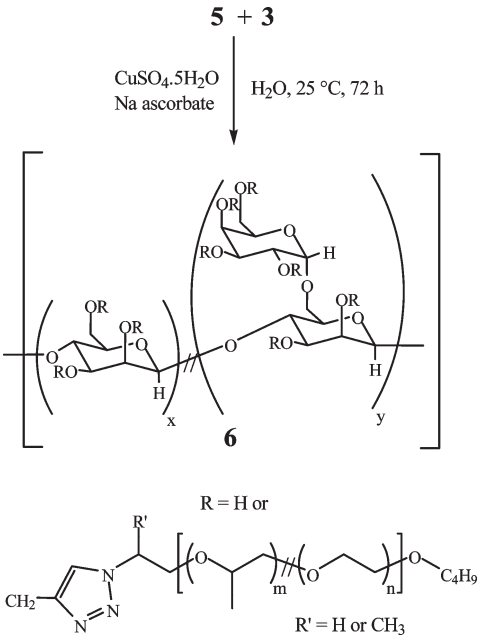

yield a very notable hydrolysis of mesylate chain ends leading to ω-OH−PEO-*co*-PPO starting material. The success of the azide functionnalization was evidenced by ^{13}C NMR with the absence of signals from mesylate and hydroxyl chain ends expected at 38.0 ppm and 64.6−66.3 ppm respectively as well as with the appearance of the characteristic signals of azide chain ends at 55.9−56.6 ppm (Figure S6). Also, the success of the ω-OH−PEO-*co*-PPO derivatization was qualitatively confirmed by the appearance of the characteristic absorption band at 2100 cm^{-1} in the FTIR spectra. SEC traces evidenced the absence of chain ends coupling reactions, resulting in a well-defined ω-N_3−PEO-*co*-PPO **3** (Figure S7).

Synthesis of Guar-Based Grafted Copolymers by CuAAC. The grafted guar-based copolymers were prepared in water at 25 °C via the CuAAC reaction by simply mixing in water, sodium ascorbate, copper(II), alkyne-functionalized guar chains $\mathbf{5_{a-c}}$ and ω-N_3−PEO-*co*-PPO **3** (Scheme 2). Given the LCST value of ω-N_3−PEO-*co*-PPO **3** similar to the one of PEO-*co*-PPO precursor (50 °C, experimentally confirmed through turbidity measurements), the click coupling reaction was performed at room temperature, which led to transparent homogeneous solutions. The resulting grafted copolymers, guar-*g*-(PEO-*co*-PPO) $\mathbf{6_{a-c}}$, were purified by dialyzis followed by freeze-drying.

The grafted copolymers were characterized by ^{1}H NMR and the success of the click coupling was clearly evidenced by the peak at 8.09 ppm characteristic of the 1,4-disubstituted 1,2,3-triazole rings (denoted proton 1 in Figure 1). The degree of substitution of guar in PEO-*co*-PPO side-chains were determined from thermogravimetric analysis (see Table 1 and Figure S8). This method is well-suited and reliable for the calculation of DS with side-chains of relatively high molar mass, as for polyoxyalkylene grafts used in this work. The DS values (Table 1) determined from this method were found to be close to the DS_{alkyne} of the corresponding alkyne-functionalized guar precursors, determined from NMR analysis, which reflects the CuAAC efficiency for the preparation of guar-*g*-(PEO-*co*-PPO) and its quantitative character.

From available alkyne-functionnalized guar derivatives $\mathbf{5_{a,b,c}}$ and taking advantage of this well controlled CuAAc

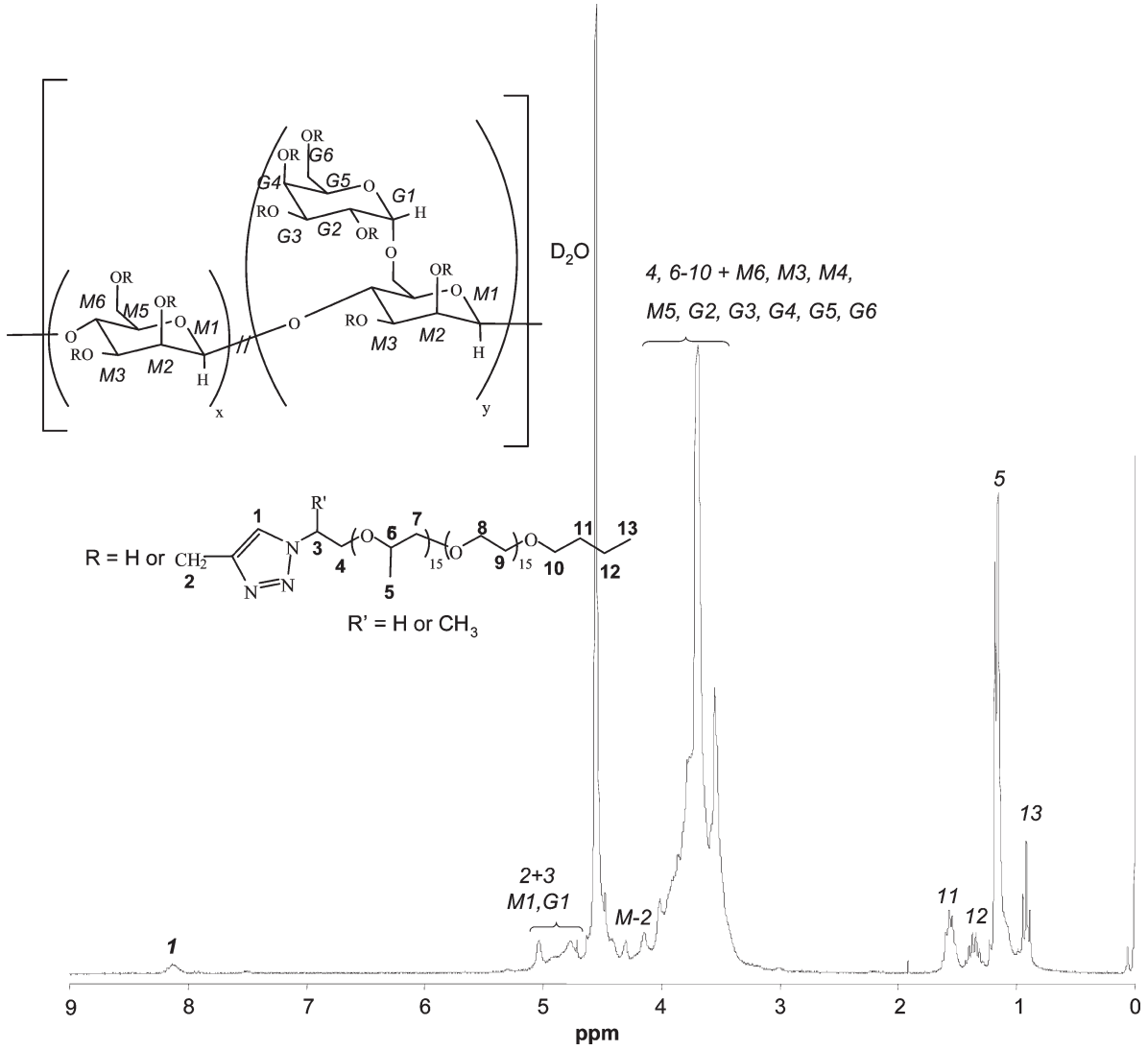

Figure 1. ^{1}H NMR spectrum of guar-*g*-(PEO-*co*-PPO) $\mathbf{6_{a0.06}}$ (D_2O, 10 mg/mL, 25 °C).

Table 2. Characteristic of the Guar Precursor Aqueous Solutions $\mathbf{4_{a-c}}$ at 25 °C

guar M_w (kg/mol)	$[\eta]$ (mL/g)	C^* (g/L)	Z
58	105	9.5	5.2
126	186	5.4	9.3
299	346	2.9	17.3

coupling, we have varied the chemical composition of the grafted copolymers, leading to a panel of samples with various guar molecular weight ranging from 58 kg/mol to 299 kg/mol and different DS values varying from 0.04 to 0.16. By this way, the average number of thermosensitive graftings per one guar chain (f) can be tuned from 10 to 150 (see Table 1).

Rheological Characterization of Guar-Based Grafted Copolymers Aqueous Solutions. For all samples, rheological measurements were conducted on copolymers with a constant concentration of the guar backbone of 50 g/L which allowed for the investigation of the behavior in semidilute entangled regime since 50 g/L $\gg C^*$ which corresponds to the overlap concentration (see Table 2). The overlap concentrations C^* were deduced from the intrinsic viscosity assuming that $C^*[\eta]$ is about unity[41] and the intrinsic viscosities were determined according to the Mark−Houwink−Sakurada parameters ($[\eta] = 0.038 \times M_w^{0.723}$) obtained by Cheng et al.[29] for the same experimental conditions. The Z values given in Table 2 correspond to the degree of chain overlapping for a guar solution at 50 g/L estimated from $Z \approx C[\eta]$.[27] In this concentration range, the associations between PEO-*co*-PPO side-chains mainly rely on interchain interactions and according to the Z values, additional guar chain entanglements could be expected to govern the rheological properties in addition to the intermolecular PEO-*co*-PPO junctions.

Table 1. Structural Characteristics of the Grafted Copolymers $\mathbf{6_{a-c}}$

expt	guar M_w kg/mol	wt % of **3** in the copolymer[a]	DS[b]	f[c]
$\mathbf{6_{a0.06}}$	58	37	0.06	10
$\mathbf{6_{b0.04}}$	126	28	0.04	15
$\mathbf{6_{b0.12}}$	126	54	0.12	50
$\mathbf{6_{b0.16}}$	126	61	0.16	65
$\mathbf{6_{c0.06}}$	299	37	0.06	60
$\mathbf{6_{c0.11}}$	299	52	0.11	110
$\mathbf{6_{c0.15}}$	299	60	0.15	150

[a] Weight fraction of **3** in the grafted copolymers determined by TGA. [b] Degree of substitution of guar in PEO-*co*-PPO side chains determined by TGA. [c] Average number of grafted PEO-*co*-PPO side chains per guar backbone. f = (*guar* $M_n \times$ DS)/162 where 162 g/mol corresponds to the molar mass of one anhydroglucose unit of guar.

Evidence of Thermoassociative Properties. Figure 2 depicts the viscoelastic properties from dynamic studies performed

on an aqueous solution of guar-*g*-(PEO-*co*-PPO) $\mathbf{6_{b0.12}}$ at 99 g/L, solicited at a constant frequency of 1 Hz with a heating rate of 1 °C/min until 90 °C to limit the water evaporation. A strain amplitude of 10% was used to ensure that the measurement was taken in the linear viscoelastic regime. The thermogram clearly shows three temperature domains. From 15 to 50 °C, the elastic G' and loss G'' moduli continuously decrease upon heating and G'' is greater than G'. It is typical of native guar behaving as a viscoelastic fluid for which viscoelastic properties decrease when temperature increases due to the progressive dissociation of intermolecular hydrogen bonding. In this temperature range, the PEO-*co*-PPO side-chains are below their LCST and thus soluble in water. From 50 to 73 °C, both G' and G'' sharply increase of around three decades. From 50 °C, the PEO-*co*-PPO side-chains start to self-associate to form interchain hydrophobic junctions which strongly affect the resulting rheological properties. The temperature from which an increase of viscoelastic properties is observed, denoted temperature of association T_{assn}, can be correlated to the LCST (around 50 °C) of the PEO-*co*-PPO grafts.

From 67 °C (Figure 2), G' becomes greater than G'', suggesting that the grafted copolymer solution behaves as a physical network composed of dehydrated PEO-*co*-PPO hydrophobic domains. In a first approximation, the temperature corresponding to the crossover $G' = G''$ can be rightly considered as an indicator of the sol−gel transition temperature (T_{gel}).[27,42] Thus, T_{gel} of guar-*g*-(PEO-*co*-PPO) $\mathbf{6_{b0.12}}$ at 99 g/L is 67 °C. The maximum G' value reached at $T = 73$ °C (denoted T_{max}) a value of 300 Pa which reflects a more elastic physical gel compared to other polysaccharide-based thermoassociative networks ($G' < 100$ Pa).[17,20,27] From 73 °C, the G' and G'' values decrease with a G' value which remains above G''. As previously described for poly(acrylic acid)-*g*-POE,[7] we can assume that, from 73 °C, a more important fraction of PEO-*co*-PPO side-chains is involved into the formation of hydrophobic zones which provides very large domains causing a weakening of the network due to a phase separation of the grafted copolymer solution.

The superimposition of the viscoelastic response under heating and cooling demonstrates (i) the reversibility of the thermoassociation process without pronounced hysteresis effect and (ii) the stability of guar chains for this temperature range. The very weak difference in the G' and G'' values at low temperature can be explained by a slight water evaporation.

The thermo-induced transition from a viscoelastic liquid to a physical gel-like behavior was also evidenced by the rheological data collected from the frequency dependence of G', G'' and complex viscosity η^* at three temperatures (25, 70, 75 °C) (Figure 3), in each temperature domain.

(i) Below T_{assn}, i.e., at 25 °C, the η^* is quasi Newtonian on the whole frequency range explored, and the storage modulus G' smaller than G'' reflects a fluid behavior of the copolymer solution.

(ii) At 70 °C, very close to the sol−gel transition temperature ($T_{gel} = 67$ °C), the G' and G' moduli are of similar magnitudes and follow relatively close frequency dependence, which is typical of the transition between liquid-like and solid-like behaviors.

(iii) At 75 °C, G' is larger than G'' from 0.1 to 10 Hz, which reflects a physical network-type structure on this explored range of frequency. However, the G' and G'' moduli are not totally constant but decrease at low frequencies which highlights the overall relaxation of the system with the time. The characteristic longer relaxation time τ_c, obtained from the inverse of the frequency corresponding to the crossover point of G' and G'' is not distinguishable anymore, indicating a slowing down of the dynamics which is mainly induced by the formation of interchain PEO-*co*-PPO associations. We can notice also that the PEO-*co*-PPO self-association involves a strong increase of complex viscosity η^* for low frequencies, combined to a strong shear-thinning effect, compared to the one observed at 25 °C.

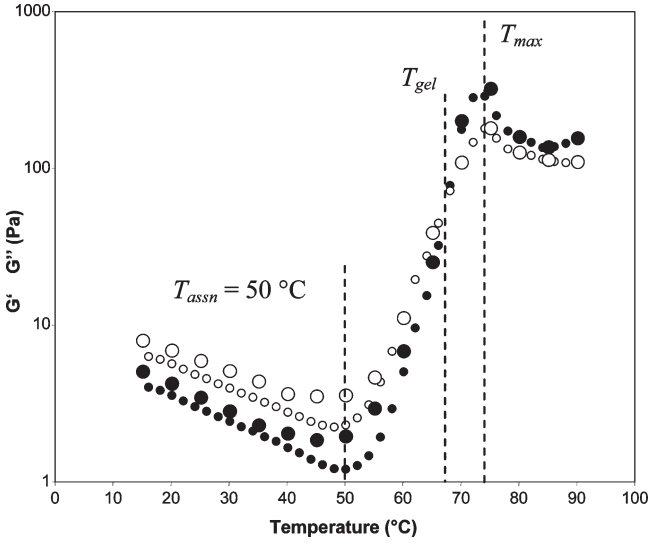

Figure 2. Variation of G' (●) and G'' (○) moduli with temperature for a guar-*g*-(PEO-*co*-PPO) solution $\mathbf{6_{b0.12}}$ in pure water ($C_{copolymer} = 99$ g/L; $f = 1$ Hz) upon heating (small symbols) and cooling (large symbols) (heating rate = 1 °C/min).

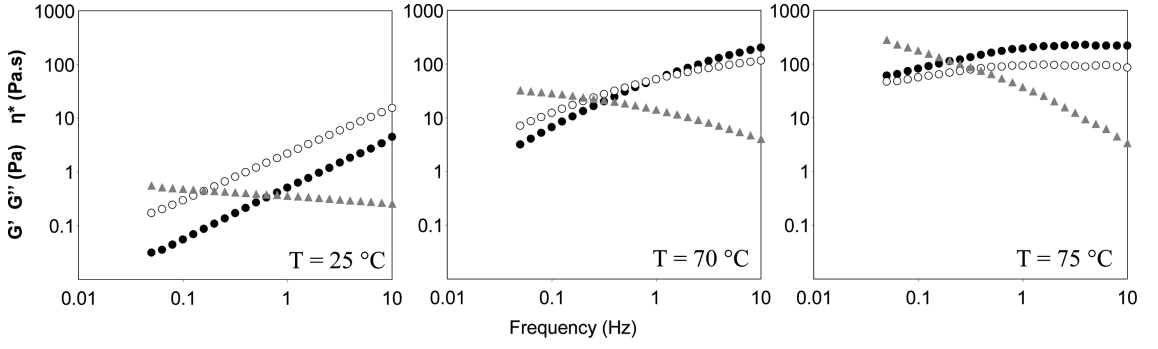

Figure 3. Frequency dependence of G' (●) and G'' (○) moduli and η^*(gray dot) for a guar-*g*-(PEO-*co*-PPO) solution $\mathbf{6_{b0.12}}$ in pure water ($C_{copolymer} = 99$ g/L, $f = 1$ Hz) at 25 (left), 70 (middle) and 75 °C (right).

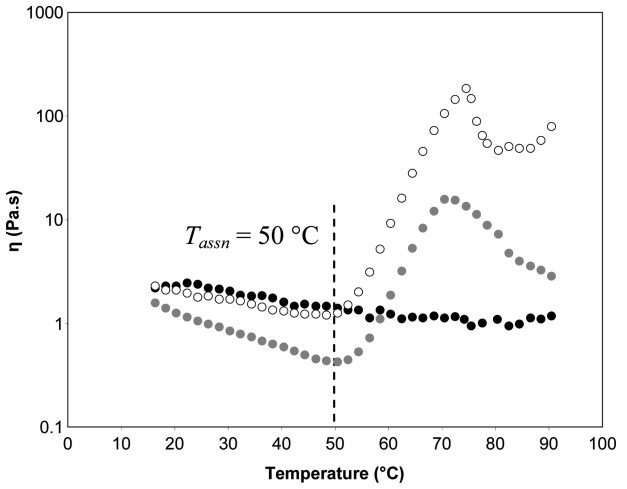

Figure 4. Variation of viscosity with temperature for native guar solutions $\mathbf{4_b}$ (●) (C_{guar} = 50 g/L, 0.05 s^{-1}) and guar-*g*-(PEO-*co*-PPO) solutions $\mathbf{6_{b0.12}}$ ($C_{copolymer}$ = 99 g/L and C_{guar} = 50 g/L) in pure water at two different imposed shear rates: 0.05 s^{-1} (○) and 1 s^{-1} (gray dot) (heating rate = 1 °C/min).

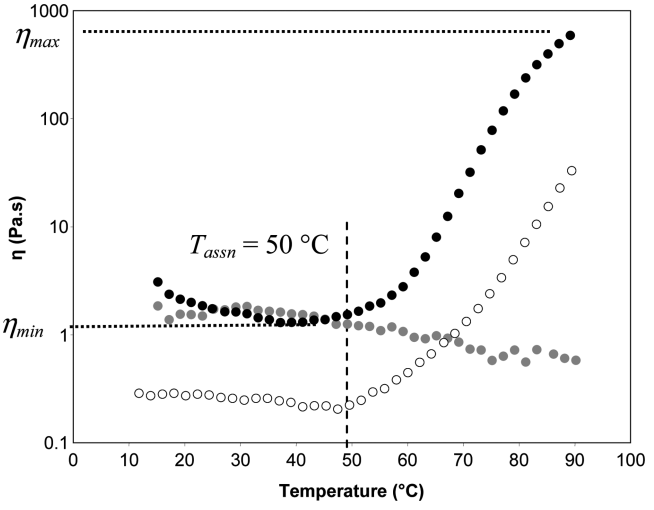

Figure 5. Variation of viscosity with temperature for guar-*g*-(PEO-*co*-PPO) solutions in pure water ($C_{copolymer}$ = 75 g/L and C_{guar} = 50 g/L): $\mathbf{6_{a0.06}}$ (gray dot); $\mathbf{6_{b0.04}}$ (○); $\mathbf{6_{c0.06}}$ (●)) (0.05 s^{-1}; heating rate = 1 °C/min).

The thermoassociative properties of the guar-*g*-(PEO-*co*-PPO) solution $\mathbf{6_{b0.12}}$ at 99 g/L was also investigated through the monitoring of the thermo dependent steady shear viscosity response for two different imposed shear rates (0.05 and 1 s^{-1}), compared to the behavior of the unmodified guar precursor at 50 g/L (Figure 4).

For the guar solution $\mathbf{4_b}$, the shear flow curve displays a continuous decrease of viscosity on the whole range of temperature, according to a typical Arrhenius' law (E_a = 12.5 kJ/mol). The grafted copolymer $\mathbf{6_{b0.12}}$ clearly shows the expected thermothickening properties with a T_{assn} around 50 °C in agreement with the previous dynamic measurements. From T_{assn}, the side-chains start to self-associate intermolecularly leading to hydrophobic domains reflected by the sharp and continuous viscosity increase of two decades on around 20 degrees. The reversibility of the thermothickening process was verified, which confirms the thermodynamic equilibrium (data not shown). Also, we can notice that the behavior of the $\mathbf{6_{b0.12}}$ solution depends on the imposed shear

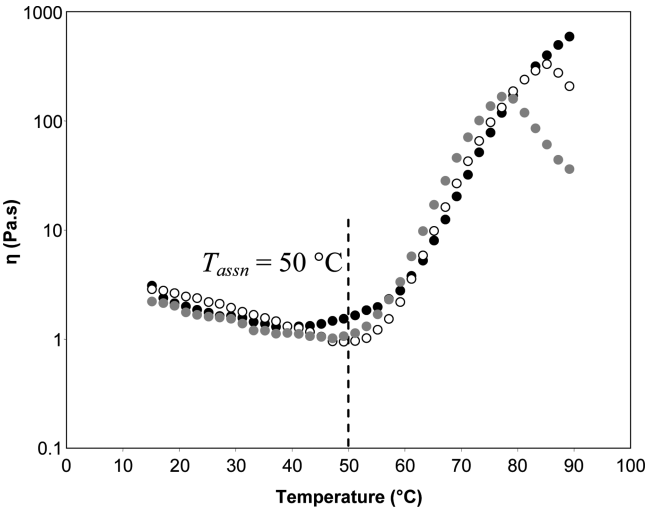

Figure 6. Variation of viscosity with temperature for guar-*g*-(PEO-*co*-PPO) solutions in pure water: $\mathbf{6_{c0.06}}$ (●; $C_{copolymer}$ = 75 g/L); $\mathbf{6_{c0.11}}$ (○; $C_{copolymer}$ = 99 g/L); $\mathbf{6_{c0.15}}$ (gray dot; $C_{copolymer}$ = 124 g/L). C_{guar} = 50 g/L for all samples (0.05 s^{-1}; heating rate = 1 °C/min)..

rate related to its shear thinning properties which comes from (i) guar chains disentanglement for $T < T_{assn}$ and (ii) guar chains disentanglement combined to the reversible dissociation of weak hydrophobic interactions for $T > T_{assn}$.

Influence of the Guar Molecular Weight. The rheological properties of the grafted copolymers are expected to depend on the guar molecular weight. Its influence was conducted by keeping guar concentration constant (around 50 g/L), via the profile of steady shear viscosity versus temperature of three guar-*g*-(PEO-*co*-PPO) solutions: $\mathbf{6_{a0.06}}$, $\mathbf{6_{b0.04}}$, $\mathbf{6_{c0.06}}$ corresponding to a precursor guar chain of M_w = 58 kg/mol, 126 kg/mol and 299 kg/mol respectively (Figure 5). The DS of guar in PEO-*co*-PPO side-chains of these three samples is nearly the same, which implies a constant PEO-*co*-PPO weight fraction within the grafted copolymer (around 30 wt %).

From Figure 5, the $\mathbf{6_{a0.06}}$ solution behaves as the unmodified guar and does not exhibit a thermothickening effect. This molecular weight (M_w = 58 kg/mol) at this guar concentration (C_{guar} = 50 g/L) leads to a very low degree of chain overlapping (Z = 5.2, Table 1) combined with a low PEO-*co*-PPO content per guar chain (f = 10, Table 1), which are unfavorable to the formation of interchain association of PEO-*co*-PPO side chains, as already observed for PAA-*g*-PNIPAAm solution at low concentration.[8] In such conditions, the association process rather occurs via a homomolecular way. Thus, a minimum number of PEO-*co*-PPO grafts per chain is required to the physical network establishment.

Conversely, the T_{assn} for the two copolymers $\mathbf{6_{b0.04}}$ and $\mathbf{6_{a0.06}}$ is the same, i.e. around 50 °C, which again demonstrates that, as described with synthetic backbones,[8] the final association temperature is closely fixed by the cloud point of PEO-*co*-PPO solubilized in the same solvent and experimental conditions.

For all the temperature range, the viscosity of the $\mathbf{6_{b0.04}}$ solution is smaller than the $\mathbf{6_{c0.06}}$ in agreement with the lower molecular weight of the guar precursor. The magnitude of the thermothickening effect can be reflected through the η_{max}/η_{min} ratio, where η_{max} is the maximal viscosity reached at high temperature and η_{min} is the smallest viscosity attained (Figure 5). This ratio is enhanced by the guar backbone length increase. Indeed, the higher the M_w is, the higher entanglement degree and the interchain associations are. In addition, for high f values, a more important fraction of

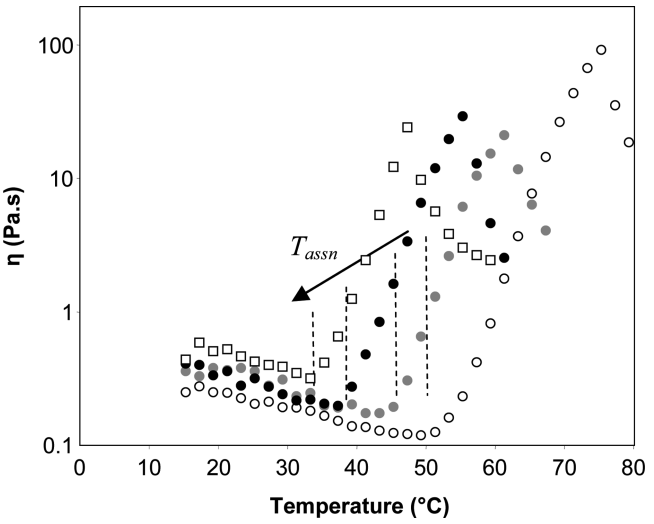

Figure 7. Variation of viscosity with temperature for guar-*g*-(PEO-*co*-PPO) solutions $\mathbf{6_{b0.12}}$ ($C_{copolymer}$ = 99 g/L and C_{guar} = 50 g/L) in pure water (○) and in presence of NaCl: 0.5 mol/L (gray dot), 1 mol/L (●), and 1.5 mol/L (□) (0.05 s^{-1}; heating rate = 1 °C/min)..

elastically active chains PEO-*co*-PPO is involved into the hydrophobic domains.

Influence of DS of Guar in PEO-co-PPO Side-Chains. The rheological response of copolymers $\mathbf{6_{c0.06,0.11,0.15}}$ (M_w = 299 kg/mol) was investigated. They only differ by their graft content (DS = 0.06, 0.11 and 0.15), leading to increasing average numbers of PEO-*co*-PPO stickers per guar chain: 60, 110, and 150 respectively (Figure 6).

The T_{assn} value remains constant (50 °C) for the three guar derivatives which is consistent with the PEO-*co*-PPO cloud point and with its low variation with concentration.

Conversely, we can notice that both the magnitude of the thermothickening effect as well as the magnitude of the thermo-induced phase separation are affected by DS variations. Surprisingly, the lowest DS appears as optimal (among the three tested) and provides the best properties in term of thermo-induced viscosity increase with no demixtion on the explored temperature range. The increase of the modification extent plays on the association process by increasing the number and the size of aggregations. Thus, for higher DS, as described for chitosane derivatives,[21] the interchain hydrophobic domains are too strongly strengthened and generate an unexpected phase separation, reflected by the viscosity drop. It appears more adapted to increase the guar molecular weight, compared to the DS of guar, to efficiently and selectively control the magnitude of the thermoviscosifying effect. The same conclusions were drawn for experiments involving copolymers $\mathbf{6_{b0.04}}$, $\mathbf{6_{b0.12}}$, and $\mathbf{6_{b0.16}}$ (data not shown).

Influence of Salt Concentration. In order to tune the thermoresponsive properties without changing the chemical nature of the synthetic side-chains grafted onto guar backbone, the impact of salt concentration was investigated on guar-*g*-(PEO-*co*-PPO) $\mathbf{6_{b0.12}}$ solutions (Figure 7).

It clearly appears that salt addition can be considered as an external trigger to easily tune the T_{assn} of the grafted copolymer since this critical temperature notably decreases with a NaCl concentration increase (43 °C, 39 and 32 °C for NaCl at 0.5 M, 1 and 1.5 M respectively). This phenomena, well-known as "salting-out" effect is ascribed to the polyoxyalkylene solubility decrease in salt conditions,[7] which promotes the PEO-*co*-PPO deshydratation and thus its hydrophobic self-association. It thus confirms that T_{assn} of grafted copolymers is governed by the thermodynamic properties of PEO-*co*-PPO. Although the thermo-induced association is retained, the salt addition leads to a slight lowering of the thermothickening magnitude combined to a separation phase enhancement, related to the too large intensification of hydrophobic PEO-*co*-PPO interactions in bad solvent conditions.

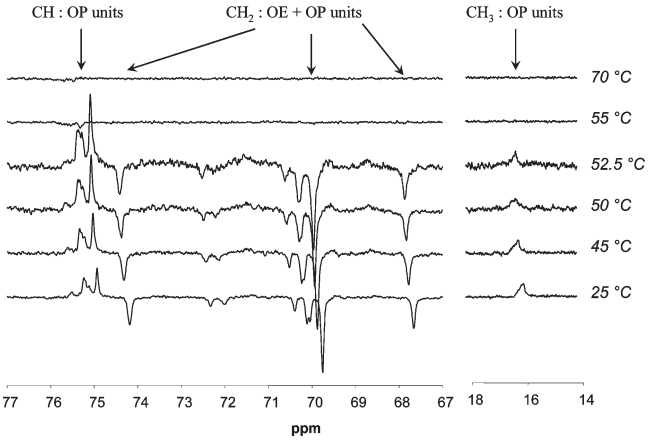

Figure 8. DEPT 135 spectra of a guar-*g*-(PEO-*co*-PPO) solution $\mathbf{6_{b0.12}}$ (D_2O, $C_{copolymer}$ = 99 g/L and C_{guar} = 50 g/L) at different temperatures.

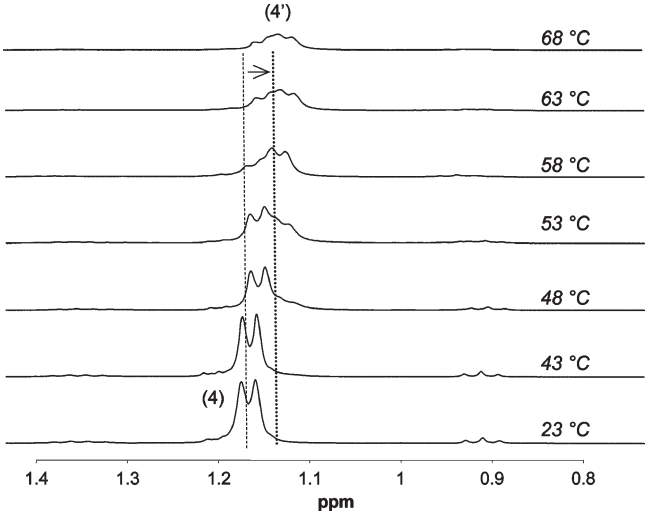

Figure 9. Effect of the temperature on the resolution of the ^{1}H NMR signal of methyl protons from PO units of a guar-*g*-(PEO-*co*-PPO) solution $\mathbf{6_{b0.12}}$ (D_2O, C_{guar} = 20 g/L).

Evidence of the Thermoassociation Process by NMR. The NMR spectroscopy can be used to study the molecular interactions and is particularly adapted to analyze the thermally generated phase transition of LCST polymers in solution.[43] The monitoring of DEPT 135 experiments of the $\mathbf{6_{b0.12}}$ solution ($C_{copolymer}$ = 99 g/L and C_{guar} = 50 g/L) at various temperatures is depicted in Figure 8. It appears that for both, guar and PEO-*co*-PPO side-chains, no carbon signals can be discerned above 55 °C.

Indeed, for this concentration condition which is the same as the one used for rheological measurements, the strong hydrophobic PEO-*co*-PPO self-associations at 55 °C yields a frozen system with a "glassy" structure which drastically restricts the overall mobility. The thermoassociation was proven to be completely reversible since after a heating cycle, DEPT 135 spectrum collected at 25 °C exhibits the expected carbon signals from guar and PEO-*co*-PPO side-chains. The

evolution observed in Figure 8 is consistent with the T_{assn} (LCST) of the guar-*g*-(PEO-*co*-PPO) determined through the macroscopical rheological analysis and the physical network-like behavior revealed by dynamic measurements (Figure 2).

To evaluate the influence of the copolymer concentration on the thermally induced aggregation at the molecular level, the same guar-*g*-(PEO-*co*-PPO) copolymer $\mathbf{6_{b0.12}}$ was analyzed at lower concentration (C_{guar} = 20 g/L) by ^{1}H NMR at temperatures ranging from 23 to 68 °C. Figure 9 displays a zoom on the intrinsic probe methyl protons region at 1.16 ppm from PO units.

From Figure 9, the change of the methyl protons signal is continuous over the explored temperature range and the signal of (CH_3) (marked as 4) of PO units at 23 °C constantly broadens. As explained for DEPT measurements, the broadening originates from the pronounced quenching of side-chain motions and the change is particularly visible above 48 °C which corresponds to the LCST of PEO-*co*-PPO. Contrary to works reported by Halacheva et al.,[44] the gradual broadening of the methyl signal upon heating, demonstrates that the improvement of guar solubility with temperature, is not sufficient to overcome the thermo-induced PEO-*co*-PPO self-associations to predominate on the final behavior. Also, the signal is gradually substituted by a weak 0.05 ppm down-shifted signal (marked as 4′), allocated to the change of local environment related to the conformation change of the PPO segment during its hydrophobic self-association. The PO moieties aggregation is also reflected by the progressive decrease of the area of the peaks upon heating due to the increased fraction of aggregated PEO-*co*-PPO. Additionally, we can notice that the triplet signal of the methyl protons of the end-butoxy groups of the PEO-*co*-PPO (at 0.92 ppm) progressively disappears upon heating.

Conclusion

Novel well-defined biohybrid thermoassociative guar-based grafted copolymers have been successfully synthesized by "grafting onto" method through the CuAAC coupling in aqueous medium. Taking advantage of this efficient, versatile and aqueous chemoselective ligation pathway, a large range of guar-*g*-(PEO-*co*-PPO) was obtained with various chemical compositions and no noticeable degradation of the guar backbone. The grafted copolymers, in semidilute regime solutions, exhibit a thermo-induced thickening resulting in a reversible physical gelation. The association temperature is mainly governed and controlled by the thermodynamic properties of the PEO-*co*-PPO grafted onto guar chains. The settlement of elastically active interchain hydrophobic PEO-*co*-PPO self-association is promoted when the guar precursor molecular weight increases, related to the higher overlapping degree and higher number of responsive stickers per guar chain. The grafting extent was proved to have an important influence upon the association process by playing on the size and number of aggregations. It results that optimal properties were obtained for the smallest substitution degree. The salt addition appears as a convenient tool to selectively tune both the magnitude of the thermoviscosifying effect and the association temperature without necessarily changing neither the nature of the side chains nor the characteristics of the grafted copolymers. The coil−globule transition mediated by temperature variation was highlighted by ^{1}H and DEPT NMR experiments through the monitoring of their quenching motions. This versatile approach could be easily extended to the grafting onto guar chains of other water-soluble graftings, because of the efficiency, robustness, and orthogonality of the CuAAc coupling.

Acknowledgment. The authors gratefully acknowledge the financial support from Rhodia and W. Bzducha for fruitful discussions.

Supporting Information Available: Figures showing chemical structures, ^{1}H and ^{13}C NMR spectra, HBMC plots, SEC traces, and TGA analyses and text giving the general procedure of the determination of the degree of substitution. This material is available free of charge via the Internet at http://pubs.acs.org.

References and Notes

(1) L'Alloret, F. U.S. Patent US 7,115,255, 2001.
(2) Bahamdan, A.; Daly, W. H. *Polym. Adv. Technol.* **2007**, *18*, 652.
(3) Fleury, E.; Tizzotti, M.; Destarac, M.; Labeau, M.-P.; Hamaide, T.; Drockenmuller, E. Patent WO2009/063082 A1.
(4) Bhattarai, N.; Ramay, H. R.; Gunn, J.; Matsen, F. A.; Zhang, M. *J. Controlled Release* **2005**, *103*, 609.
(5) Drury, J. L.; Mooney, D. J. *Biomaterials* **2003**, *24*, 4337.
(6) Hourdet, D.; L'Alloret, F.; Audebert, R. *Polymer* **1997**, *38*, 2535.
(7) Hourdet, D.; L'Alloret, F.; Durand, A.; Lafuma, F.; Audebert, R.; Cotton, J.-P. *Macromolecules* **1998**, *31*, 5323.
(8) Durand, A.; Hourdet, D. *Macromol. Chem. Phys.* **2000**, *201*, 858.
(9) Hourdet, D.; Gadgil, J.; Podhajecka, K.; Badiger, M. V.; Brûlet, A.; Wadgaonkar, P. P. *Macromolecules* **2005**, *38*, 8512.
(10) Barbier, V.; Hervé, M.; Sudor, J.; Brûlet, A.; Hourdet, D.; Viovy, J.-L. *Macromolecules* **2004**, *37*, 5682.
(11) Petit, L.; Karakasyan, C.; Pantousier, N.; Hourdet, D. *Polymer* **2007**, *48*, 7098.
(12) Lee, B. H.; Song, S.-C. *Macromolecules* **2004**, *37*, 4533.
(13) Ahn, S.; Ahn, S. W.; Song, S.-C. *Colloids Surf., A* **2009**, *333*, 82.
(14) Liang, D.; Zhou, S.; Song, L.; Zaitsev, V. S.; Chu, B. *Macromolecules* **1999**, *32*, 6326.
(15) Hasan, E.; Jankova, K.; Samichkov, V.; Ivanov, Y.; Tsvetanov, C. B. *Macromol. Symp.* **2002**, *177*, 125.
(16) Chung, H. J.; Bae, J. W.; Park, H. D.; Lee, J. W.; Park, K. D. *Macromol. Symp.* **2005**, *224*, 275.
(17) Seetapan, N.; Mai-ngam, K.; Plucktaveesak, N.; Sirivat, A. *Rheol. Acta* **2006**, *45*, 1011.
(18) Chung, H. J.; Go, D. H.; Bae, J. W.; Jung, I. K.; Lee, J. W.; Park, K. D. *Curr. Appl. Phys.* **2005**, *5*, 485.
(19) Bhattarai, N.; Matsen, F. A.; Zhang, M. *Macromol. Biosci.* **2005**, *5*, 107.
(20) Creuzet, C.; Auzély-Velty, R.; Rinaudo, M. *Actual. Chim.* **2006**, *294*, 34.
(21) Auzély-Velty, R.; Creuzet, C. Patent WO2009/034130 A1.
(22) Ohya, S.; Nakayama, Y.; Matsuda, T. *Biomacromolecules* **2001**, *2*, 856.
(23) Cho, K. Y.; Chung, T. W.; Kim, B. C.; Kim, M. K.; Lee, J. H.; Wee, W. R.; Cho, C. S. *Int. J. Pharm.* **2003**, *24*, 83.
(24) Kitazono, E.; Kaneko, H. Patent EP1659143 A1.
(25) Bokias, G.; Mylonas, Y.; Staikos, G.; Bumbu, G. G.; Vasile, C. *Macromolecules* **2001**, *34*, 4958.
(26) Hourdet, D.; L'Alloret, F.; Audebert, R. *Polymer* **1997**, *38*, 2535.
(27) Karakasyan, C.; Lack, S.; Brunel, F.; Maingault, P.; Hourdet, D. *Biomacromolecules* **2008**, *9*, 2419.
(28) Tizzotti, M.; Charlot, A.; Fleury, E.; Stenzel, M.; Bernard, J. *Macromol. Rapid Commun.*, DOI:10.1002/marc.201000072.
(29) Cheng, Y.; Brown, K. M.; Prud'homme, R. K. *Biomacromolecules* **2002**, *3*, 456–461.
(30) Tayal, A.; Pai, V. B.; Khan, S. A. *Macromolecules* **1999**, *32*, 5567–5574.
(31) Gliko-Kabir, I.; Yagen, B.; Penhasi, A.; Rubinstein, A. *Pharm. Res.* **1998**, *15*, 1019–1025.
(32) Cunha, P. L. R.; Castro, R. R.; Rocha, F. A. C.; Feitosa, J. P. A. *Macromol. Symp.* **2008**, *266*, 48–52.
(33) Coviello, T.; Alhaique, F.; Dorigo, A.; Matricardi, P.; Grassi, M. *Eur J. Pharm. Biopharm.* **2007**, *66*, 200–209.
(34) Sandolo, C.; Matricardi, P.; Alhaique, F.; Coviello, T. *Eur. Polym. J.* **2007**, *43*, 3355–3367.
(35) Mercuri, D.; Leone, G.; Barbucci, R.; Favaloro, R.; Facchini, A.; Signori, F.; Bronco, S.; Ciardelli, F. *Macromo. Symp.* **2008**, *266*, 74–80.
(36) Panariello, G.; Favaloro, R.; Forbicioni, M.; Caputo, E.; Barbucci, R. *Macromol. Symp.* **2008**, *266*, 68–73.

(37) Gliko-Kabir, I.; Yagen, B.; Penhasi, A.; Rubinstein, A. *J. Controlled Release* **2000**, *63*, 121–127.
(38) Crescenzi, V.; Cornelio, L.; Di Meo, C.; Nardecchia, S.; Lamanna, R. *Biomacromolecules* **2007**, *8*, 1844–1850.
(39) Ostaci, R-V.; Damiron, D.; Capponi, S.; Vignaud, G.; Léger, L.; Grohens, Y.; Drockenmuller, E. *Langmuir* **2008**, *24*, 2732.
(40) Tizzotti, M.; Labeau, M.-P.; Hamaide, T.; Drockenmuller, E.; Charlot, A.; Fleury, E. *J. Polym. Sci. Part A: Polym. Chem.* **2010**, *48*, 2733.
(41) Macosko, C. W. G. *Rheology: Principles, Measurements and Applications*; Macosko, C. W., Ed.; VCH Publishers, Inc: Weinheim, Germany, 1994.
(42) Petit, L.; Bouteiller, L.; Brület, A.; Lafuma, F.; Hourdet, D. *Langmuir* **2007**, *23*, 147.
(43) Durand, A.; Hourdet, D.; Lafuma, F. *J. Phys. Chem. B* **2000**, *104*, 9371.
(44) Halacheva, S.; Rangelov, S.; Tsvetanov, C. *Macromolecules* **2006**, *39*, 6845.